ELSEVIER

Journal of Structural Geology 28 (2006) 220–235

JOURNAL OF STRUCTURAL GEOLOGY

www.elsevier.com/locate/jsg

The nature and importance of phyllonite development in crustal-scale fault cores: an example from the Median Tectonic Line, Japan

S.P. Jefferies [a], R.E. Holdsworth [a,*], C.A.J. Wibberley [b], T. Shimamoto [c], C.J. Spiers [d], A.R. Niemeijer [d], G.E. Lloyd [e]

[a] *Reactivation Research Group, Department of Earth Sciences, University of Durham, Durham DH1 3LE, UK*
[b] *Université de Nice-Sophia Antipolis, UMR Géosciences Azur, Les Lucioles, 06560 Valbonne, France*
[c] *Department of Geology & Mineralogy, Graduate School of Science, Kyoto University, Kyoto, Japan*
[d] *HPT Lab. Faculty of Geosciences, Utrecht University, Utrecht, the Netherlands*
[e] *Department of Earth Sciences, University of Leeds, Leeds, UK*

Received 2 June 2005; received in revised form 7 October 2005; accepted 19 October 2005
Available online 15 December 2005

Abstract

Like many large, crustal-scale faults, the Median Tectonic Line (MTL) in SW Japan has a long history of movement, having been active predominantly as a strike-slip fault since the mid-Cretaceous. Fault rock exposures in the core of the MTL preserve a history of deformation at a range of mid- to shallow-crustal depths. Ryoke mylonites 1–4 km north of the main contact record deeper level, Cretaceous top-to-the-south sinistral movements. The remainder of the fault zone core is surprisingly narrow, exhibiting a wide variety of fault rocks that illustrate both the interaction and effects of syn-tectonic fluid influx over a range of deformation conditions. Exposures within 50 m of the central slip zone display a progressive sequence in fault rock evolution from ultramylonite → cataclasite → foliated cataclasite → phyllonite → breccia/gouge. This sequence occurs because cataclasis in the vicinity of the fault core creates permeable pathways for the ingress of chemically active fluids into the fault zone. This leads to the replacement of load-bearing phases, such as feldspar, by fine-grained, foliated aggregates of intrinsically weaker phyllosilicates such as white mica and chlorite. The grain size reduction associated with both cataclasis and mineral alteration creates conditions ideal for the operation of fluid-assisted, stress-induced diffusive mass transfer mechanisms. Comparison with the findings of recent experimental studies suggest that the fault zone processes observed in the core of the MTL will lead to long-term weakening, provided the network of phyllosilicate-rich fault rocks are able to form an interconnected thin layer of weak material on kilometre- to tens of kilometre-length scales.

Keywords: Phyllonite; Fault zone weakening; Diffusive mass transfer; Fluid-assisted alteration; Median Tectonic Line; Japan

1. Introduction

Many crustal-scale fault and shear zones repeatedly localise displacements on various timescales, but the mechanical significance of such heterogeneous deformation is controversial, especially for the frictional regime in the upper crust (e.g. Rutter et al., 2001). It is generally believed that such faults must be weak relative to adjacent regions of intact rock. Many authors argue that geophysical measurements of surface heat flow and stress orientations associated with crustal-scale structures such as the San Andreas Fault indicate a more fundamental fault weakening in an absolute sense, i.e. these discontinuities are characterised by anomalously low frictional strengths (e.g. Lachenbruch and Sass, 1980; Zoback, 2000). There is a lack of consensus, however, and others have argued that such faults are in fact strong (e.g. Scholz, 2000). Part of the problem is that most of the geophysical techniques used to address these problems lack sufficient spatial resolution to identify the possible causes of weakening along the principal displacement surfaces/zones that lie within fault cores, which are typically <1 km thick (Holdsworth, 2004).

Geological studies of fault rock microstructures give an insight into the evolution of deformation mechanisms and

* Corresponding author. Tel.: +44 191 3342299; fax: +44 191 3342301.
E-mail address: r.e.holdsworth@durham.ac.uk (R.E. Holdsworth).

0191-8141/$ - see front matter © 2006 Elsevier Ltd. All rights reserved.
doi:10.1016/j.jsg.2005.10.008

rheological behaviour of fault zones at different depths (e.g. Schmid and Handy, 1991; Snoke et al., 1998). Studies that have focused on fault rocks formed in the upper crust (<5 km depth) have proposed that weakening may be caused by several mechanisms. These include the presence of anomalously low-friction clay gouges (e.g. Wang, 1984; Morrow et al., 1992), the development of high fluid overpressures (e.g. Byerlee, 1990; Rice, 1992; Chester et al., 1993) or dynamic mechanisms such as thermal pressurisation of fluids or frictional melting (e.g. Hickman et al., 1995). However, there is often a paucity of direct geological evidence to support these theories (Scholz, 1990) and it seems unlikely that they can account for long-term weakening and reactivation of continental basement faults (e.g. Holdsworth et al., 2001).

More recently, field-based research (e.g. Imber et al., 1997, 2001; Stewart et al., 2000; Gueydan et al., 2003; Collettini and Holdsworth, 2004; Wibberley, 2005) has focused on major faults where exhumation has exposed fault rocks formed at depths closer to the frictional–viscous (or brittle–ductile) transition. In this depth range, rocks potentially preserve evidence of the weakening mechanisms that operate where faults cut through the main load-bearing region of the crust, e.g. between 5 and 15 km. These studies, together with others of shear zone localisation and development in granitoid rocks deformed under low greenschist facies conditions (e.g. Mitra, 1984; Janecke and Evans, 1988; Shea and Kronenberg, 1992; Chester et al., 1993; Goodwin and Wenk, 1995; Wintsch et al., 1995; Hippertt, 1998; Wibberley, 1999) have suggested that the development of cohesive foliated phyllosilicate-rich fault rocks—or phyllonites—which overprint early cataclasites may be fundamentally important. There is an increasing body of experimental data (e.g. Shea and Kronenberg, 1993; Bos and Spiers, 2002; Niemeijer and Spiers, 2005) demonstrating that such phyllonites are potentially very weak.

The present study focuses on the development of phyllonites in the core region of the Median Tectonic Line (MTL), SW Japan (Fig. 1a) and presents both geological field-based and microstructural observations. The MTL in this location was chosen for study because a diverse assemblage of exhumed fault rocks deformed across the frictional–viscous transition are exposed at the surface.

2. Geological setting and structure of the Median Tectonic Line

The MTL is a major, crustal-scale fault in Japan that separates the low-P/high-T Ryoke metamorphic belt of subduction related granitoids with subordinate metasedimentary rocks from the high-P/low-T Sambagawa belt of accretionary complex metasedimentary rocks (Fig. 1a). It has an onshore along-strike length of >1000 km, with a displacement history reaching back at least to the early Cretaceous. Displacement estimates are uncertain and range between 200 and 1000 km (e.g. Ichikawa, 1980). The

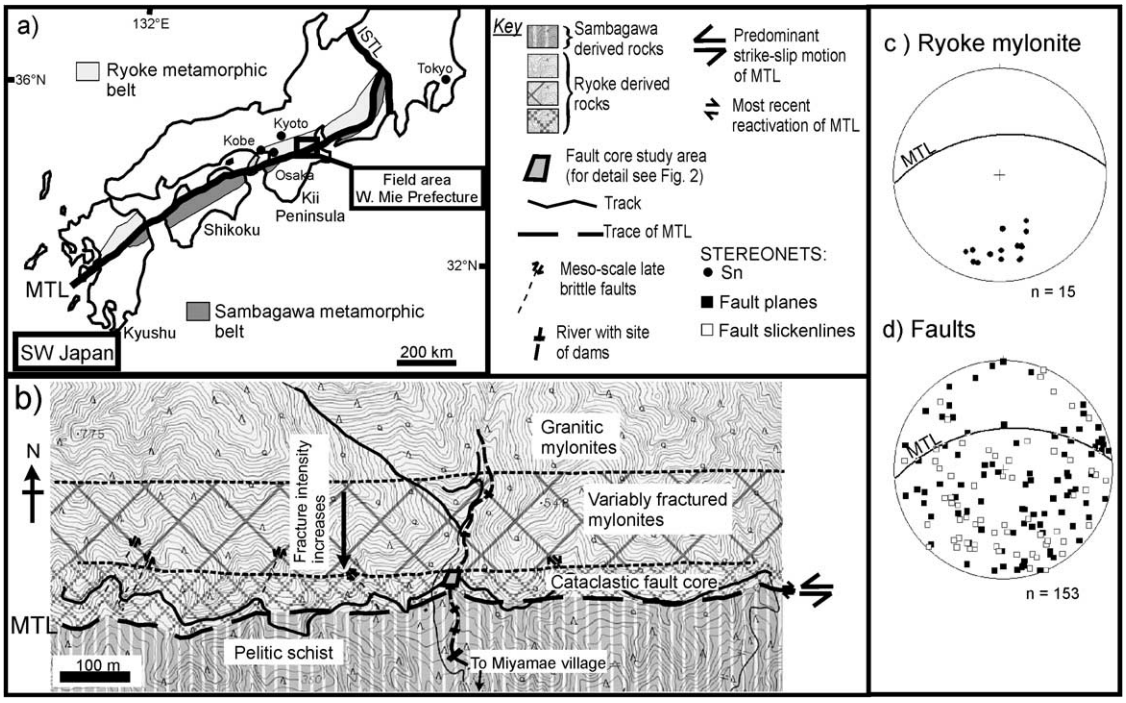

Fig. 1. (a) The Median Tectonic Line (MTL) in SW Japan showing adjacent metamorphic belts. ISTL = Itoigawa–Shizuoka Tectonic Line. (b) Geological map of the MTL near Miyamae village, western Mie Prefecture. (c) Stereonet showing poles to Ryoke mylonite foliation (Sn). (d) Stereonet showing poles to meso-scale fault planes and fault slickenlines. The stereograms are lower-hemisphere equal-area stereographic projections, all data collected 350–60 m N of MTL central slip zone (CSZ).

granitic Ryoke belt rocks are variably mylonitised in a zone up to 5 km wide north of the MTL and formed during late Cretaceous to mid-Tertiary sinistral movements. Exhumation during continued activity and reactivation of the fault has resulted in the current exposure of the fault zone displaying a wide variety of fault rocks generated at different levels in the mid- to upper-crust. Deformation associated with these sinistral displacements becomes increasingly brittle as the central part (hereafter referred to as the 'core') of the fault is approached with the development of cataclasites, breccias and gouges, many of which are foliated (e.g. Takagi, 1985, 1986; Wibberley and Shimamoto, 2003).

The MTL at the surface has a dip of around 60°N but geophysical evidence suggests that the fault shallows to around 35° from the surface to about 5 km depth (Ito et al., 1996). Previous studies in Mie Prefecture have suggested that the fault has primarily undergone sinistral strike-slip displacements (e.g. Ichikawa, 1980; Takagi et al., 1989; Ohmoto, 1993; Shimada et al., 1998). However, the MTL has recently been reactivated as a dextral strike-slip fault (Sugiyama, 1992), with displacements localized into incohesive fault rocks typically within a couple of metres of the central slip zone (e.g. Wibberley and Shimamoto, 2003).

2.1. Structural history and protoliths

Two contrasting protoliths occur either side of the MTL—Ryoke belt granitoids to the north and Sambagawa belt semi-pelitic schist to the south. Formation of the high-angle MTL and sinistral strike-slip displacements occurred during the early Tertiary (e.g. Hara et al., 1980; Ichikawa, 1980; Ohmoto, 1993 and references therein). Outside of this region of sinistral shear, the Ryoke granitoids in a zone up to 5 km wide are thought to preserve evidence of mylonitisation that occurred during an earlier late Cretaceous to earliest Tertiary sinistral top-to-the-south, sub-horizontal shearing event that pre-dates the formation of the high-angle MTL (Yamamoto and Masuda, 1987; Michibayashi and Masuda, 1993; Ohmoto, 1993). The granitic mylonites have a mean grain size of ~0.5 mm and are composed of quartz, K-feldspar, plagioclase, hornblende and biotite. Quartz veins are common, are often discontinuous and range in size from the centimetre- to metre-scale. Detailed studies of the

Table 1
Showing textural and mineralogical changes with decreasing distance to the MTL central slip zone (CSZ). Compiled from field observations, optical microscopy, SEM and whole-rock XRF analyses. UM = indicates location of ultramylonite on the northern edge of the fault core, ←P→ = indicates location of phyllonitic overprint within the fault core. (= note that the white mica content partly appears to decrease from ultramylonite to phyllonite due to the large increase in precipitated chlorite in the latter unit)

	VARIABLY FRACTURED MYLONITES					FAULT CORE	
Distance N of CSZ	350 m	300 m	250 m	200 m	150 m	100 m	50 m UM ← P → 0
Grainsize mm	0.45	0.4		0.12	0.8	0.03	0.01 <1.5
Hornblende + biotite %	5%	2.5%		<2%	<1.5%	0%	Absent
White mica %	2%	3-4%		4%	7%	30%	*8%
Chlorite %	5%	5%		6%	8%	10%	30%
K-feldspar : albite ratio	50:50	45:55		42:58	40:60	No K-feld'	
Veining	cm-scale epidote veins extensive			cm-scale epidote & calcite		Extensive cm-scale calcite veins	
Lineation	Weak elongated quartz			Weak elongated quartz		Very strong chlorite lineation	
Foliation	Weak	Good flattening & elongation of grains		Strong flattening of grains		Very strong grain flattening &chlorite alighnment	
Intensity of feldspar cataclasis	Mild	Mild with alteration of K-feld' to white mica		Extensive		Less fracturing of remaining albite, more alteration to white mica	
Intensity of faulting/ cataclasis	Weak fracturing	Weak fracturing		Widespread	Fracture & fault intensity increases	Strong intensive cataclasis	

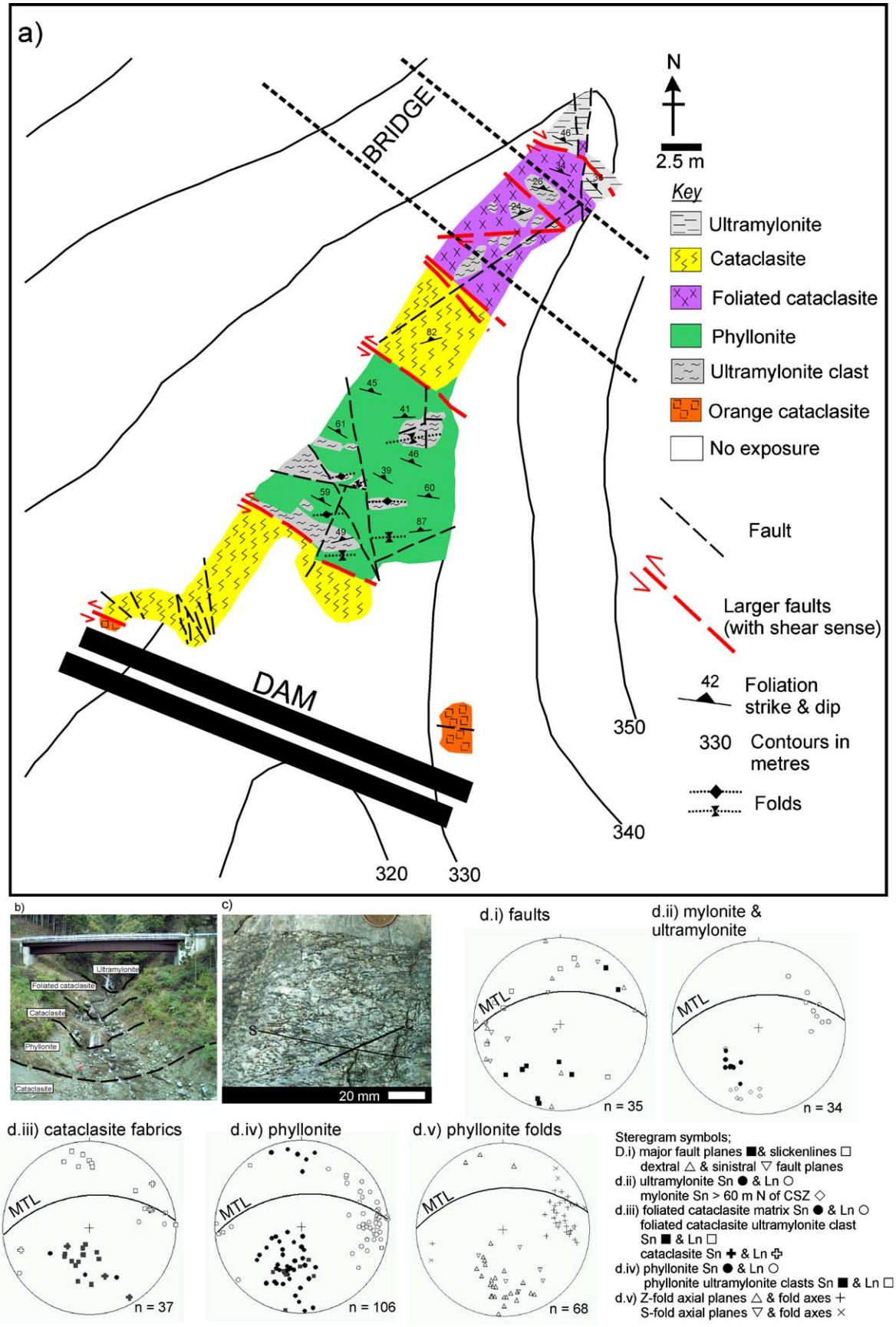
a)
BRIDGE
DAM
N
2.5 m
Key
Ultramylonite
Cataclasite
Foliated cataclasite
Phyllonite
Ultramylonite clast
Orange cataclasite
No exposure
Fault
Larger faults (with shear sense)
42 Foliation strike & dip
330 Contours in metres
Folds
350
340
320
330
b)
Ultramylonite
Foliated cataclasite
Cataclasite
Phyllonite
Cataclasite
c)
S
C
20 mm
d.i) faults
MTL
n = 35
d.ii) mylonite & ultramylonite
MTL
n = 34
d.iii) cataclasite fabrics
MTL
n = 37
d.iv) phyllonite
MTL
n = 106
d.v) phyllonite folds
MTL
n = 68
Steregram symbols;
D.i) major fault planes ■& slickenlines □
dextral △ & sinistral ▽ fault planes
d.ii) ultramylonite Sn ● & Ln ○
mylonite Sn > 60 m N of CSZ ◇
d.iii) foliated cataclasite matrix Sn ● & Ln ○
foliated cataclasite ultramylonite clast
Sn ■ & Ln □
cataclasite Sn ✚ & Ln ✜
d.iv) phyllonite Sn ● & Ln ○
phyllonite ultramylonite clasts Sn ■ & Ln □
d.v) Z-fold axial planes △ & fold axes +
S-fold axial planes ▽ & fold axes ×

Ryoke mylonitic rocks are presented by Hayama and Yamada (1980), Takagi (1985) and Shimada et al. (1998).

The Sambagawa protolith to the south of the MTL is a semi-pelitic schist composed primarily of quartz, white mica and feldspar (albite). The schist is very fine-grained, with albite forming primarily as porphyroblasts set within a fine-grained quartz–mica matrix, with a grainsize of <0.2 mm. The petrology (e.g. Enami et al., 1994), geochronology (e.g. Dallmeyer et al., 1995) and structural evolution (e.g. Hara et al., 1980; Wallis et al., 1992) of the Sambagawa belt are all well characterised.

The MTL *fault core* is here defined by the zone of intense brittle deformation and alteration related to the formation of cataclasite- and phyllosilicate-rich fault rocks during steeply dipping strike-slip motion along the faulted contact between the Ryoke and Sambagawa belts. The cataclastic deformation overprints earlier mylonites and is interpreted as having formed during continuous strike-slip deformation at progressively shallower crustal conditions (Takagi, 1986). The distribution of deformation in the core is highly asymmetric in the wall-rock protoliths. On the northern side of the MTL, the fault core is $\sim$50 m wide and a zone of variably fractured and faulted granitic mylonites continues for a further 200–250 m northwards (Fig. 1b). Within the Sambagawa rocks, however, foliated cataclastic fault rocks occur in a poorly exposed zone <15 m wide.

3. MTL structure and fault rocks, Mie Prefecture

3.1. MTL fault zone structure in the Miyamae village area

The present study focuses on the well-exposed fault rocks on the northern side of the MTL, which are derived from Ryoke protoliths in the region above Miyamae village, Iitaka-cho, Matsusaka-shi, Mie Prefecture (Fig. 1b). Ryoke granitic mylonites exposed at distances >300 m north of the central slip zone (Fig. 1b) have a mean grain size of $\sim$0.45 mm and contain both K-feldspar and plagioclase (albite after andesine–oligoclase) porphyroclasts, set in a matrix of feldspars, quartz, hornblende and biotite. There is some alteration of the feldspars to white mica, and hornblende and biotite to chlorite. The mylonitic foliation trends east–west (086), with an average dip of 61°N (Fig. 1c), and a mineral lineation is occasionally seen moderately plunging toward the east (Takagi, 1985; Shimada et al., 1999). Ductile microstructures including asymmetrically wrapped feldspar porphyroclasts and oblique foliations developed in recrystallized quartz aggregates everywhere suggest sinistral reverse senses of shear (Shimada et al., 1999).

At distances less than 300 m north of the central slip zone, the earlier mylonitic textures are progressively overprinted by cataclastic deformation (Table 1). From a distance of 100 m, faults are widespread and have a wide array of orientations (Fig. 1d) and are mutually cross-cutting so that no specific generations of faulting can be defined. The highly faulted core begins 50 m north of the central slip zone and is well exposed in the north–south-trending Fukaya River section (Fig. 2a and b). Cataclastic fault rocks derived from ultramylonite are predominant, but foliated cataclasites and phyllonites are also present. Located 2 m north of the central slip zone, a distinctive orange-stained cataclasite occurs that is extremely altered with no original mylonitic features or textures preserved. Within the fault core, epidote veins are no longer visible, but centimetre-scale carbonate veining becomes extensive (Table 1).

The central slip zone, or plane of most recent slip, is a 1-cm-wide gouge that cross-cuts all other structures. The plane strikes east–west (085) and dips 59° towards the north. The gouge is extremely fine grained with SEM studies revealing a quartz, feldspar, kaolinite, chlorite, smectite and occasionally illite mineralogy (Takagi, 2005, personal communication). Orange- and black-coloured incohesive foliated cataclasites and gouges occur for approximately 2 m either side of the central slip zone and are composed of quartz, calcite, white mica and chlorite. All these fault rocks locally preserve evidence for dextral Riedel shears and asymmetrical tails deflected around larger clasts (cf. Wibberley and Shimamoto, 2003).

The Sambagawa-derived rocks south of the MTL are poorly exposed and comprise a narrow, <15-m-wide zone of foliated gouge and cataclasite composed primarily of quartz, white mica and opaque carbonaceous material.

3.2. Fault rocks of the MTL core: the Fukaya River Section

3.2.1. Faults

Brittle faults often form the boundaries between different fault rock units exposed in the stream section and in some cases are marked by steep scarps and waterfalls (Fig. 2a and b). Most bigger faults strike ESE, oriented at a low angle to the MTL central slip zone with moderate to steep northward dips. Where visible, slickenlines consistently indicate oblique sinistral motion with downthrows to the north (Fig. 2d. i). Collectively these faults appear to cause considerable lateral variations in fault rock distributions along strike (see also Wibberley and Shimamoto, 2003). Smaller faults appear to be mutually cross-cutting and show an array of orientations and senses of shear, oriented at both

Fig. 2. (a) Simplified geological map of the MTL fault core. For further explanation see text. (b) Photograph of the river section, taken from the top of the dam looking toward the north; the orange cataclasite in the southernmost part of map in (a) is out of view. (c) Photograph of Ryoke granitic mylonite. (d) Stereograms showing structural data on faults and fault rock deformation fabrics, Sn = foliation, Ln = mineral lineation, CSZ = central slip zone. All planes are shown as poles apart from the great circle = central MTL slip surface.

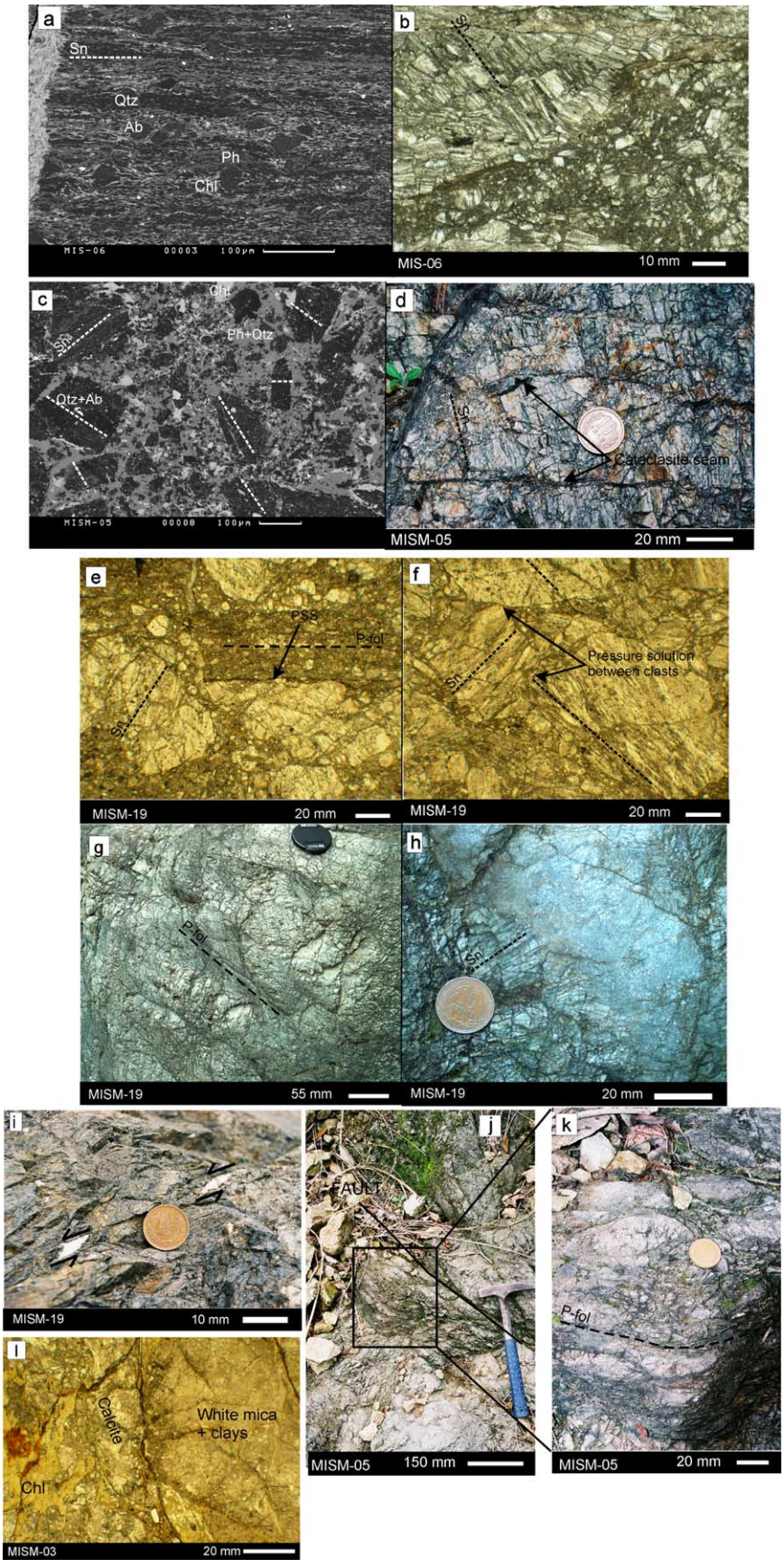
a
Sn
Qtz
Ab
Ph
Chl
MIS-06 00003 100µm
b
Sn
MIS-06
10 mm
c
Chl
Ph+Qtz
Sn
Qtz+Ab
MISM-05 00008 100µm
d
Sn
Cataclasite seam
MISM-05
20 mm
e
PSS
P-fol
Sn
MISM-19
20 mm
f
Sn
Pressure solution between clasts
MISM-19
20 mm
g
P-fol
MISM-19
55 mm
h
Sn
MISM-19
20 mm
i
MISM-19
10 mm
j
FAULT
MISM-05
150 mm
k
P-fol
MISM-05
20 mm
l
Calcite
White mica + clays
Chl
MISM-03
20 mm

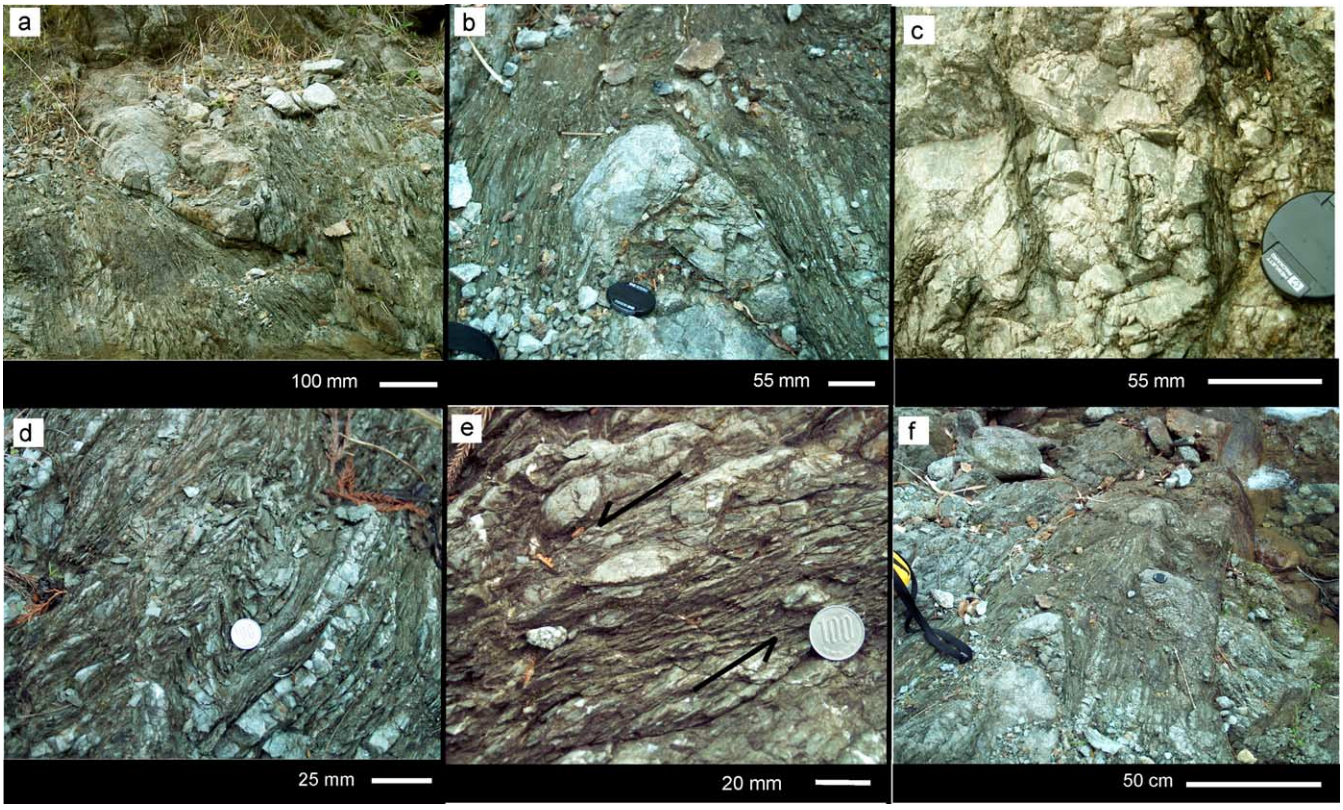

Fig. 4. Field observations of phyllonite within MTL fault core. (a) and (b) Phyllonite enveloping ultramylonite lenses. (c) Phyllonitic fabric developing along fractures through an ultramylonite lens. (d) Centimetre-scale folds within the phyllonite. (e) Sinistral shear bands. (f) Metre-scale fold, looking down fold hinge.

high and low angles to the central slip zone of the MTL (Fig. 2d.i).

3.2.2. Ultramylonite

More-or-less intact ultramylonites crop out at the northern end of the section, and are contained as relict clasts in all the other fault rock units. Hence, they are thought to form the protolith for most of the other fault rocks preserved in the section (Fig. 2a and b). The ultramylonites typically weather to a grey–dark green colour and fracturing gives the rock a blocky appearance, with little or no veining visible. Other outcrop-scale features such as shear criteria are difficult to distinguish due to the very fine-grained nature of the rock (grain size $\sim$0.01 mm), but a strong ultramylonitic foliation (mean 126/45N) defined by quartz-rich and quartz-poor domains and mineral lineation (mean 32/071) defined by the alignment of white mica and chlorite are recorded (Fig. 2d. ii).

3.2.3. Cataclasite

Pale grey–green, unfoliated cataclasites (Fig. 3d) are derived from ultramylonite and are strictly proto-cataclasites as they have $<$50% cataclasite matrix (Sibson, 1977). Two units occur either side of the phyllonite exposed in the river section (Fig. 2a and b), both being bounded by sinistral-oblique faults.

3.2.4. Foliated cataclasite

The foliated cataclasite forms a fault-bounded unit 13 m wide sandwiched between ultramylonite and cataclasite (Fig. 2a). The foliated cataclasite ($\sim$40% clast, 60% matrix) contains numerous clasts of fractured ultramylonite up to 3.5 m across, set in a fine-grained cataclasite matrix (mean grain size $<$0.5 mm). Larger clasts have been individually mapped (Fig. 2a). The foliated cataclasite matrix is dark green and clasts have a milky white colour (Fig. 3g and h). Within the matrix, a weak foliation has begun to develop and clasts are often elongated parallel to the foliation with typical aspect ratios of 2:1. The foliations in the ultramylonite clasts (mean 105/32N) and cataclasite matrix (mean 101/34N) have a similar orientation (Fig. 2d.iii). A mineral lineation defined by phyllosilicates (white mica, chlorite) is locally preserved in the foliated cataclasite (mean 17/094), whilst relict mineral lineations in ultramylonite clasts plot as two clusters

Fig. 3. Key features of ultramylonite ((a) and (b)), cataclasite ((c) and (d)), foliated cataclasite ((e)–(k)) and orange stained cataclasite (l) within the MTL fault core. (a) and (c) SEM backscatter images. (b), (e), (f) and (l) Plane polarised light thin section images. (d) and (g)–(k) Field photographs. PSS = pressure solution seams, P-fol = phyllosilicate foliation, Sn = foliation, Qtz = quartz, Ab = albite, Ph = phengite, Chl = chlorite.

plunging shallowly north (23/354) and east (22/074) (Fig. 2d.iii). Within the foliated cataclasite, centimetre-scale sinistral pull-apart structures infilled with calcite are observed (Fig. 3i). Together with the shallowly plunging lineation, these features are taken to indicate that the foliated cataclasite formed during sinistral top-to-the-south shearing along the MTL.

3.2.5. Phyllonite

In outcrop, the phyllonite has a distinctive dark green colouration due to high chlorite content and a strong ESE-striking foliation (mean 107/45N). The foliation is defined by a fine millimetre-scale compositional banding of alternating phyllosilicate-rich and quartz-feldspathic microlithons of ultramylonite, with numerous sub-parallel discontinuous very fine grained quartz-rich layers up to ~10 cm thick (Fig. 2d.iv). The latter units are thought to represent relict (i.e. pre-phyllonite formation) quartz veins (cf. the vein in Fig. 4d). Phyllonite grainsize is typically <1.5 mm. A well-preserved, shallowly eastward plunging mineral lineation is defined by the alignment of chlorites (mean 18/083) (Fig. 2d.iv). Shear criteria associated with these fabrics are consistently sinistral and include asymmetrically wrapped quartz segregations/veins and low-angle shear bands (Fig. 4e). Numerous augen and lenses of brittle fractured ultramylonite identical in appearance, composition and texture to the clasts found in the adjacent units of cataclasite occur within the phyllonite (Figs. 2a and 4a and b). The augen/lenses range in length from less than 1 cm to over 1 m and are strongly wrapped by and elongated within the main foliation, with typical aspect ratios of 11:1 (Fig. 4a and b). In general, ultramylonite foliations and lineations within the clasts have been reoriented so that they are now sub-parallel to those in the enveloping phyllonites (Fig. 2d.iv). Within many clasts, a phyllonitic foliation is localised along the traces of cross-cutting, pre-existing brittle fractures (Fig. 4c).

The phyllonite is highly folded by close to tight brittle–ductile fold structures on centimetre- to metre-scales. Dextral-verging folds dominate over sinistral-verging structures (Figs. 2d.v and 4d). Dextral folds have moderately- to steeply-dipping northward axial planes (mean 091/60N), and gently to moderately (10–50°) eastward plunging fold hinges. Brittle–ductile dextral shear bands/Riedel shears with centimetre- to metre-spacing are locally developed in areas unaffected by folding, whilst dextral faults possibly equivalent to P-shears locally offset dextrally-verging fold pairs. These late folds and dextral shears (Fig. 4d and f) are absent elsewhere in the fault zone in Miyamae. However, similar dextral structures are present in incohesive foliated cataclasites at Tsukide (Wibberley and Shimamoto, 2003).

3.2.6. Orange-stained cataclasite

The orange-stained cataclasite crops out in isolated exposures next to the dam (Fig. 2a). Its age relative to the other fault rocks exposed in the section is uncertain. The distinctive orange colour appears to result from the weathering out of iron oxide and it is relatively incohesive. Cataclasis and alteration are pervasive with few protolith features or textures recognisable. Mean grainsize is <1 cm.

3.3. Mineralogy and microstructures

3.3.1. Ultramylonite

These rocks are typically composed of quartz and albite porphyroclasts (~50 μm across) set in a matrix of very fine-grained (~10 μm) albite, quartz, phengitic white mica and chlorite. The phyllosilicate grains are strongly aligned defining the strong foliation that wraps around the porphyroclasts (Fig. 3a). Throughout many samples there are alternating chlorite-rich and white mica-rich domains. The ultramylonites are variably brecciated (e.g. Fig. 3b) with the local development of cataclasites identical in texture and composition to those found in the more internal regions of the fault core. Electron micro-probe analyses reveal that albite porphyroclasts are extensively altered to white mica of the same phengitic composition as that found within the matrix of both the ultramylonite and cataclasites. The ultramylonitic foliation is cross-cut by veins of little deformed carbonate (mainly calcite) in places intergrown with chlorite. Electron microprobe data show that the chlorite associated with the calcite veins is slightly enriched in Fe relative to the chlorite in the ultramylonite matrix.

3.3.2. Cataclasite

Mineralogically, the cataclasite and the ultramylonite are very similar. Microprobe analysis reveals that comparable varieties of Fe-rich chlorite, phengitic white mica (Fig. 5), albite, quartz and calcite occur throughout. However the albite is more extensively altered to phengite plus quartz in the cataclasites. In thin section, the cataclasite is texturally distinct, comprising angular fractured blocks of ultramylonite (ranging from ~50 μm upwards) within which small flecks of chlorite and white mica most prominently define the ultramylonitic foliation. The ultramylonite blocks typically sit within a very fine-grained (~3–10 μm) cataclasite, or locally ultracataclasite matrix. Rotation of these blocks has occurred so that the ultramylonitic foliation is often randomly oriented (Fig. 3c). The matrix is primarily composed of phengitic white mica plus comminuted quartz. Fluid-assisted mineral reactions have resulted in extensive alteration of the original mineralogy to a fine-grained aggregate of phyllosilicate (white mica, chlorite) and quartz. Chlorite aggregates also occur as infills along the numerous fractures throughout the cataclasite. In hand specimen, these often appear as thin dark seams coating fracture surfaces (Fig. 3d). Fluid infiltration appears to have been greatest in the finest grained parts of the matrix based on the distribution of secondary alteration in thin section and SEM images.

3.3.3. Foliated cataclasite

The angular and irregular shaped clasts of cataclastically-deformed ultramylonite within the foliated cataclasite are set in a fine-grained (~5 μm) matrix made up primarily of phyllosilicate (chlorite and white mica) plus some comminuted quartz. There is widespread textural evidence for the operation of pressure solution, particularly at the interfaces between clasts and matrix (e.g. Fig. 3e and f), where sub-parallel dissolution seams define the weak foliation seen in outcrop (Fig. 3g). The elongation of clasts parallel to the foliation appears to occur due to a combination of mechanical rotation and the effects of distributed extensional microfaulting (Fig. 3g).

As the foliation in the cataclasites intensifies, the rocks become progressively more phyllonitic, i.e. rich in aligned chlorite and white mica. These regions of 'proto-phyllonite' initially localise adjacent to earlier brittle fractures that cut through the cataclasites (Fig. 3j and k). The foliation is also generally more intense in the finest grained areas of cataclasite matrix.

3.3.4. Phyllonite

The strong phyllonitic foliation is defined primarily by the alignment of grains of chlorite and phengitic white mica. Chlorite locally constitutes up to 30% of the phyllonite and its grain size (reaching ~30–40 μm) is up to four times larger compared with the chlorite in fault rocks described previously. This gives the rock a distinctive green colour and a high sheen to foliation surfaces. White mica constitutes up to 8% of the phyllonite, of which approximately half formed as an alteration product from albite, occurring both wrapped around albite grains and along cleavage planes. The remainder of the phyllonite is made up of varying proportions of quartz, albite, calcite (mainly occurring in veins) and opaques. The ultramylonite microlithons and quartz-rich layers (relict quartz veins) appear much brighter in thin section and have low proportions of phyllosilicate. They have undergone intense dynamic recrystallization presumably during the earlier development of the ultramylonite. During phyllonite development, these units appear to have undergone little internal deformation other than fracturing and cataclasis.

The ultramylonite lenses are internally cataclastically deformed (Fig. 6a) and this often helps to extend and break up the lenses along the phyllonitic foliation. Fractures are infilled with calcite and chlorite, and any areas of fine-grained cataclasite matrix are replaced by fine-grained chlorite (Fig. 6b).

Compared with the fault rocks described previously, the phyllonites display much more evidence for pervasive fluid-assisted alteration and diffusive mass transfer. Albite porphyroclasts are typically brown and cloudy in appearance, as they have been partially altered to fine-grained aggregates of fibrous white mica (Fig. 7a). Microprobe analyses show that the white mica has a phengitic composition similar to that found in the ultramylonite and cataclasites (Fig. 5b). Pressure solution seams and fibrous overgrowths of white mica have developed widely adjacent to relatively more rigid porphyroclasts of albite (Fig. 7a and b). Significantly, the chlorite that defines the phyllonitic foliation contains less FeO and a much higher proportion of MgO compared with the chlorite that occurs within the ultramylonites, cataclasites and foliated cataclasites (Fig. 5a). This is consistent with the observation that the phyllonitic foliation overprints the previously formed fault rocks and suggests that a distinct, later phase of chlorite growth is associated with the phyllonite development. The highly altered albite porphyroclasts are increasingly flattened and elongated parallel to the network of chlorite grains that predominantly define the grain-scale foliation in the phyllonites. In addition, large clasts of original ultramylonite occur, often with sub-angular shapes (Fig. 7c). These clasts are predominantly composed of phengitic white mica and quartz, at least some of which is derived from the breakdown of original albite. Viewed under higher magnifications, the white mica is often clearly seen to preferentially replace albite along cleavage planes (Fig. 7d).

Chlorite grains are inter-grown with lesser amounts of phengitic white mica (at an approximate ratio of 6:1) and form anastomosing, interconnected layers on millimetre- to micrometre-scales that bound and wrap porphyroclasts and fractured lenses of ultramylonite, mirroring what is seen on the outcrop-scale. The chlorite bounding these porphyroclasts and fractured lenses defines seams <0.5 mm in width running through the phyllonite that form an

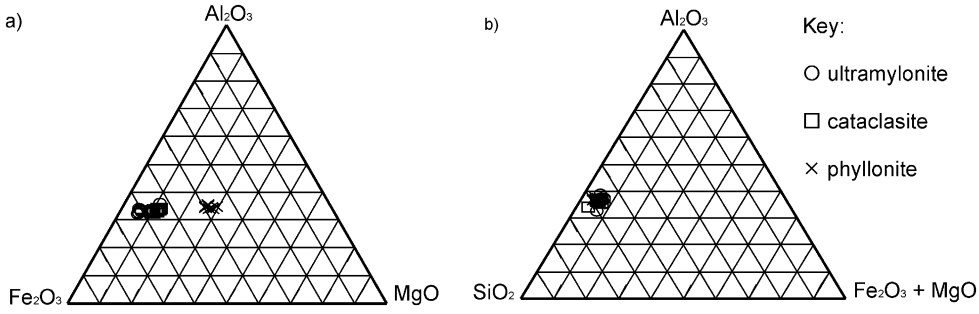

Fig. 5. Ternary diagrams to show (a) comparative Al_2O_3–Fe_2O_3–MgO content of chlorite and (b) Al_2O_3–SiO_2–Fe_2O_3 + MgO content of phengitic white mica within the MTL fault core ultramylonite, cataclasite and phyllonite. Data obtained from microprobe analyses.

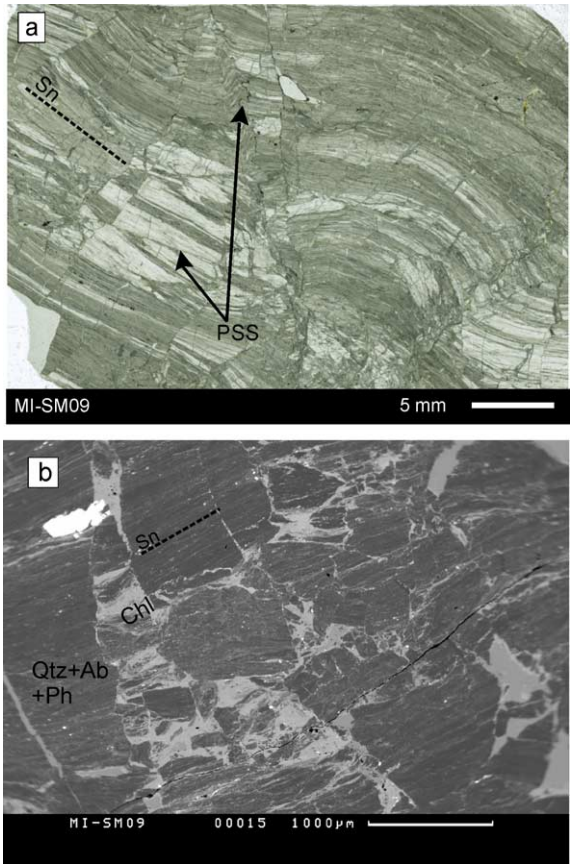

Fig. 6. Images of an ultramylonite lens within the phyllonite. (a) Plane polarised light thin section image of ultramylonite lens. (b) SEM backscatter image of fractured section of ultramylonite lens.

interconnected network or layer (Fig. 7e). Within the phyllonite, carbonate veins form at high angles (~90°) to the phyllonitic foliation, and are locally folded (Fig. 7f).

In thin section, many phyllonite samples show evidence for discrete fault-like offsets developed parallel to the main phyllosilicate foliation. Some carbonate veins are truncated or offset with dextral senses of shear when crossing chlorite-rich bands (Fig. 7g). Shearing often leads to recrystallization of carbonate grains as the veins are progressively smeared out into the foliation. There are, however, examples of cross-cutting calcite veins unaffected by such processes. Viewed in SEM, thicker bands of intergrown chlorite and white mica have locally developed millimetre- to micro-metre-scale, dextrally-verging folds (Fig. 7h). The fold hinges appear angular with kinking of individual phyllosilicate grains (Fig. 7h), suggesting semi-brittle conditions with frictional slip along phyllosilicate-foliae.

3.3.5. Orange-stained cataclasite

In thin section, few features are observed due to the extremely highly altered nature of the cataclasite (Fig. 3l), although a few relict ultramylonitic textures are locally preserved. The rock is heavily altered to very fine-grained (~5 μm) alteration products including white mica and clay minerals at the expense of albite. Carbonate (calcite, siderite, dolomite) and chlorite veining is observed on centimetre- to millimetre-scales.

3.4. Major element geochemistry

XRF whole-rock major-element analyses of selected fault rocks collected from the Fukaya River section were carried out to assess what changes in bulk geochemistry occur with fault rock evolution subsequent to the early mylonitisation associated with the MTL (Fig. 8). These data illustrate a coherent series of chemical changes that are consistent with the observed changes in fault rock mineralogy as one passes from ultramylonite to cataclasite and ultimately phyllonite. There are significant gains in Fe_2O_3, MgO and LOI and decreases in Na_2O and SiO_2 that are likely related to the breakdown of anhydrous phases such as feldspar to hydrous minerals such as phengitic white mica and the widespread growth of chlorite, especially the relatively MgO-rich variety found exclusively in the phyllonites. All these changes are likely to be induced by the action of syn-tectonic fluids as they passed through the fault zone. A more detailed analysis of both major and trace element geochemical trends in the MTL will be published elsewhere.

4. Discussion

4.1. Fault rock sequence and evolution

A complex fault rock sequence is associated with the development of the MTL, reflecting the interplay of deformation mechanisms under changing P–T conditions, fluid influx, textural feedback processes and ongoing changes in mineralogy (Table 2). The earliest fault rocks associated with MTL deformation in the Ryoke belt are mylonites (Hayama and Yamada, 1980; Takagi, 1985). Lineations are generally shallowly plunging, suggesting that strike-slip movements are dominant and shear criteria are uniformly sinistral. Using quartz microstructures, lattice preferred orientations and geothermometry, Sakakibara (1995) concluded that mylonitisation of the Ryoke granitoids occurred over a temperature and pressure range of 470–350 °C and 4–5 Kb, broadly equivalent to lowermost amphibolite to upper greenschist facies. He also proposed that, during their formation the mylonites were exhumed from approximately 18 to 11 km depth. The localised preservation of fibrous overgrowths in some ultramylonite samples (Fig. 3a) may indicate that the onset of diffusion mechanisms was triggered by grainsize reduction due to dynamic recrystallization (cf. White et al., 1980; Schmid and Handy, 1991).

The ultramylonite developed close to the MTL fault core has subsequently undergone cataclasis, presumably at lower temperatures and pressures. The microstructural evidence

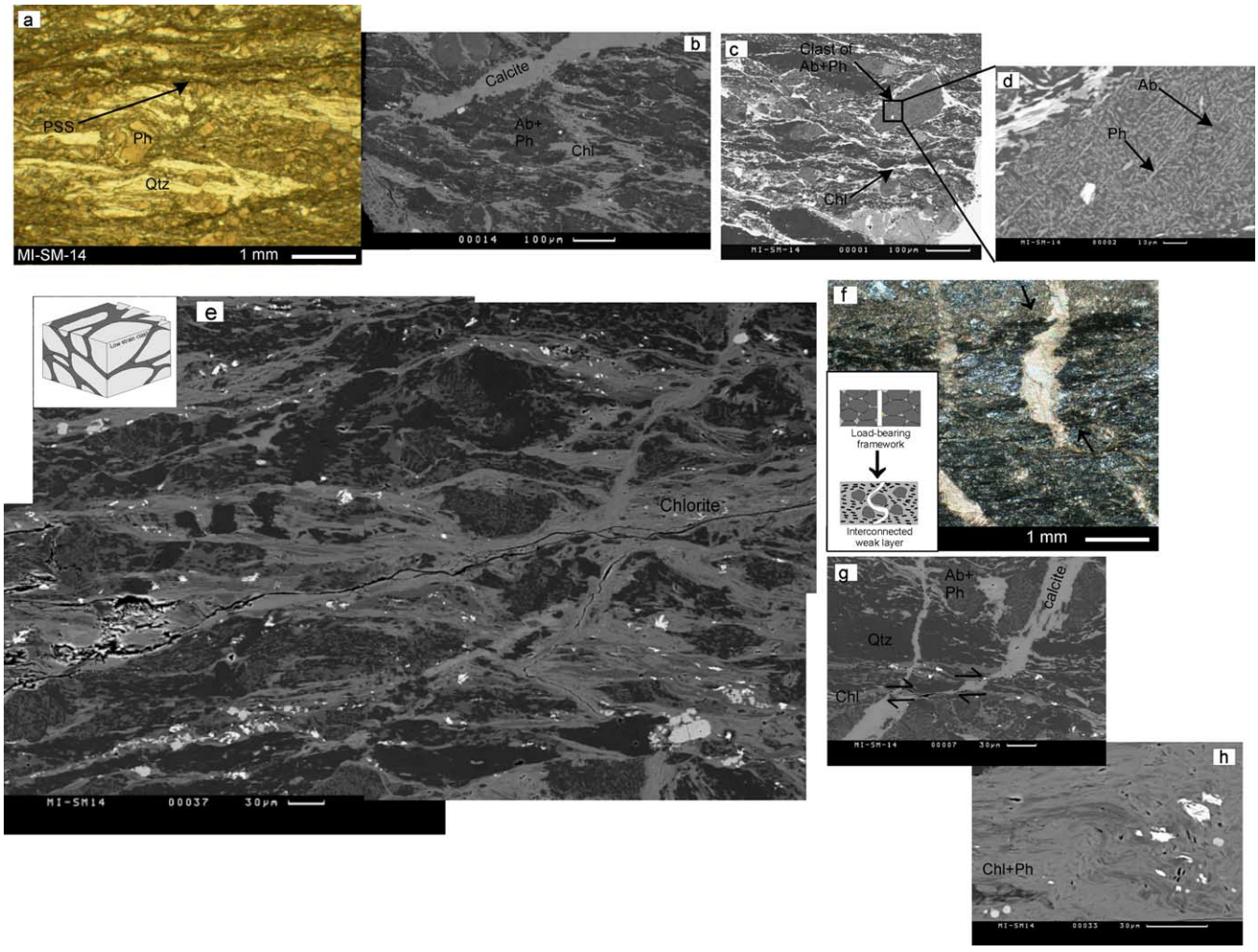

Fig. 7. Microstructural observations of phyllonite within MTL fault core. (a) Plane polarised light thin section image. (b)–(e), (g) and (h) SEM backscatter images. (f) Cross polarised light thin section image.

from thin section and SEM studies, together with the observed major element geochemical trends, suggest that focused influx of fluid into the fault core has occurred. This was presumably facilitated by fracturing and grain-scale dilatancy during cataclasis. This influx appears to have been

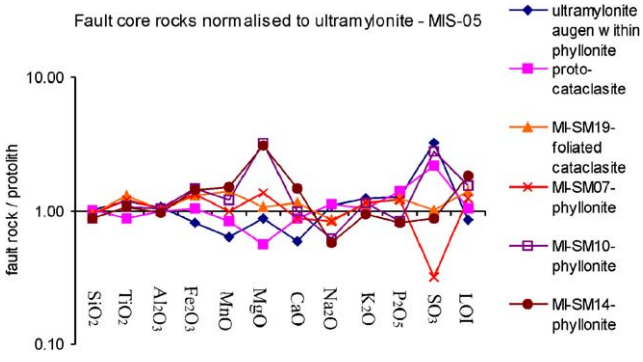

Fig. 8. Plot showing XRF whole-rock major-element analyses for the main representative fault rock types from the MTL fault core normalised relative to ultramylonite, the earliest recognised rock in the fault core.

greatest in the finest grained regions of cataclasite matrix and in regions along and immediately adjacent to pre-existing brittle fractures. As a result, phyllosilicate precipitation and the development of phyllonitic fabrics initially localises within those sections of the fault core more affected by cataclastic deformation, as illustrated on centimetre scales by the textures preserved in the foliated cataclasite of the MTL fault core. It is proposed that further fluid influx and phyllosilicate precipitation eventually converted the foliated cataclasite into phyllonite.

In parallel with the progressive alteration of fault rocks, fluid-assisted diffusive mass transfer increasingly begins to operate within the cataclasite as it evolves into phyllonite. Characteristic source microstructures, e.g. pressure solution seams and grain dissolution features, and sink microstructures, e.g. fibrous mineral overgrowths, are widely preserved. Such stress-induced dissolution and precipitation processes are likely to have been triggered by the fine grain sizes in crushed-up cataclasites and by the presence of an active fluid phase. It is likely to have been enhanced still

Table 2
Summary table to show the sequence of fault rock deformation within the MTL fault core, the associated deformation mechanisms, metamorphic processes and their rheological implications. μfn = coefficient of friction

	MYLONITE	ULTRAMYLONITE	CATACLASITE	FOLIATED CATACLASITE	PHYLLONITE	MESO-SCALE FAULTING	CSZ & GOUGE
MOVEMENT SEQUENCE	1	2	3	4	5 & 8	3-7	8
KINEMATICS	← Sinistral shear →				Late dextral reactivation →		
DOMINANT DEFORMATION MECHANISMS	Crystal plasticity	Crystal plasticity & grain boundary sliding	Cataclasis	Cataclasis, DMT, cataclasis, fracture & frictional sliding μfn = 0.6-0.8	DMT & frictional sliding μfn = ~0.2	Fracture & frictional sliding μfn = 0.6-0.8 →	
METAMORPHIC PROCESSES		Enhanced fluid influx →					
		Breakdown of anhydrous phases i.e. Albite to white mica →				Dismembering fault rock units	
					New growth of Mg-rich chlorite →		
RHEOLOGY				Reaction softening & weakening due to onset of DMT →			
				Frictional-viscous behaviour inferred →			

further by the growth of new, fine-grained secondary mineral phases during alteration. Importantly, the localisation of alteration and the onset of fluid-assisted diffusional mechanisms adjacent to pre-existing fractures and fine-grained zones of cataclasis allow the rapid development of interconnected layers of phyllosilicate on all scales (e.g. Figs. 4a and 7c and e).

A number of fluid-assisted retrograde metamorphic reactions are likely to have played an important role in the development of the MTL fault rock suite. Most significantly the Ryoke granitic mylonites 350–100 m north of the central slip zone contain both K-feldspar and albite in approximately equal proportions. Combined optical mineralogical and SEM studies of samples collected in the fault core—including the ultramylonites—indicate that K-feldspar is no longer present and that all the feldspar remaining is of an albitic composition. This suggests either that the protolith has a more tonalitic composition close to the MTL core (Ito, 1978), or that albitisation of the K-feldspar has occurred, along with phengite production (e.g. Van Staal et al., 2001), or that K-feldspar breakdown to phengite occurred directly. In the latter two cases, the reactions most likely began synchronous with the development of the ultramylonites within the core region of the MTL due to the influx of fluids. However, microprobe and SEM studies within the cataclasites and phyllonites of the core show that phengitic white mica of essentially identical composition is also being formed due to the widespread retrograde breakdown of individual albite grains. This is consistent with the observed decrease in Na within the cataclasites and phyllonites of the fault core relative to both the ultramylonite (Fig. 8) and the wall rock Ryoke protoliths (see Table 1).

The observed sequence of fault rock overprinting implies that the K-feldspar breakdown to phengite (+albite?) accompanying development of the ultramylonites is post-dated by albite alteration to phengite to generate the phyllonites. This sequence is strikingly similar to that described by Wibberley (1999) from granitoid thrust fault zones of the Pelvoux Massif, external Western Alps, and by Van Staal et al. (2001) from the shear zones of the Spruce Lake nappe in Canada. It may be a common feature of fluid-assisted retrograde metamorphism in collision/subduction-related tectonic settings. In addition, it has already been noted that the dominant chlorite in the phyllonites has a distinctly higher Mg composition compared with that in the adjacent ultramylonite and cataclasites. It may be that the observed changes in modes of retrograde metamorphism and chlorite composition reflect changes in fluid compositions or other environmental conditions such as temperature and pressure (e.g. Cathelineau, 1988; Wintsch et al., 1995).

Several studies have shown that the most recent displacements along the MTL are dextral (e.g. Sugiyama, 1992) and that these are associated mainly with incohesive fault rocks found within a few metres of the central slip zone (e.g. Wibberley and Shimamoto, 2003). In the Fukaya river section, however, there is clear evidence that late dextral shearing has been preferentially localised into the phyllonites leading to the development of dextral folds and shear bands. Significantly, no other Ryoke-derived rock unit in

close proximity to the MTL core—other than the central slip plane—is affected by this dextral shearing. Assuming that this late movement can be correlated with the late dextral slip recognised elsewhere along the MTL, then the observed focusing of strain exclusively within the phyllosilicate-rich fault core is consistent with these rocks being weak on long timescales and under varying conditions in the upper crust (see below).

4.2. Texture and rheology of phyllonites: insights from deformation experiments

The strongly developed foliation and lineation in the MTL phyllonites and the anastomosing and coalescing nature of the fabric surrounding variably flattened porphyroclasts gives the rocks a superficially mylonitic appearance. However, optical and SEM textural studies have found little evidence for significant amounts of dynamic recrystallization or recovery having occurred in these rocks. A possible solution to this apparent enigma comes from the findings of recent experimental work that use rock analogue mixtures to assess the rheological effects of fluid-assisted diffusional mechanisms in phyllosilicate-rich fault rocks.

In a series of experimental studies, Bos and Spiers (2000, 2002), Bos et al. (2000a,b) and Niemeijer and Spiers (2005) performed ultra-high strain rotary shear experiments on simulated fault gouges consisting of halite and kaolinite or muscovite mixtures as analogues for the deformation of quartz- and mica-rich fault rocks. The experiments were carried out under temperature conditions where pressure solution and cataclasis are known to dominate over dislocation creep in halite. In wet samples with >10 wt% phyllosilicate, brittle failure was followed by strain weakening towards a steady-state shear strength that was dependent on both sliding rate and normal stress (so called 'frictional–viscous flow'). Significantly, although no crystal plasticity occurred during any of the experiments, the microstructures produced at lower sliding velocities are remarkably similar to the apparently mylonitic textures seen within the MTL phyllonites.

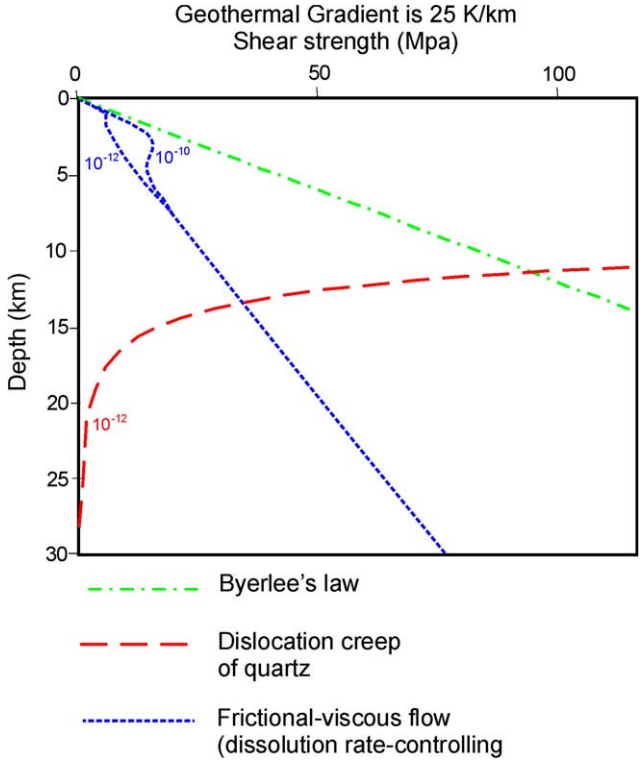

Fig. 9. Calculated strength profile for the MTL phyllonites produced by Niemeijer and Spiers (in press). Profile drawn for quartz–mica phyllonite with a quartz 'grain size' of 50 μm within a strike-slip fault.

Bos and Spiers (2002) and Niemeijer and Spiers (2005) have proposed a microphysical model in which the shear strength of the gouge undergoing steady-state flow is determined by the combined resistance to shear created by frictional sliding on the phyllosilicate foliae, pressure solution in the halite (=quartz) and dilation on the foliation. Fig. 9 is a calculated strength profile produced using this microphysical model for a strike-slip scenario comparable with the MTL phyllonite. It was drawn for a quartz–mica phyllonite with an average grain size of 50 μm. The profile has been constructed using strain rates of 10^{-10} and $10^{-12}\,s^{-1}$, equivalent to a fault zone of 10 and 1000 m width sliding at 30 mm year^{-1}. The Byerlee's Law and wet quartz dislocation creep curves used in Fig. 9 represent the 'classical' two-mechanism crustal strength profile, with the frictional–viscous transition located at $\sim$12 km depth. The frictional viscous curve derived from the experimental data predicts that the dilatant or cataclastic portion of the crust is restricted to the upper few kilometres (Fig. 9). For a strain rate of $10^{-10}\,s^{-1}$, at around 3–4 km depth, pressure solution controls slip on the foliation and a reversal in slope is predicted because the operation of pressure solution becomes easier with increasing temperature. Between 3 and 7 km, the strength accordingly falls away from the quasi-Byerlee line down toward the lower strength line representing stable-slip on the foliation with a reduced coefficient of sliding friction. Effectively this reduces the thickness of the seismogenic layer to less than 5 km. In the depth range 5–15 km, the predicted profile might even represent an upper boundary for the estimated strength of the phyllonites because, if plastic deformation by dislocation creep of the phyllosilicate were in operation, the fault rock might be even weaker (see Kronenberg et al., 1990; Shea and Kronenberg, 1992, 1993; Mares and Kronenberg, 1993; Niemeijer and Spiers, 2005).

One potential limitation to the application of the strength profile to the MTL is that many of the phyllonites contain significant amounts of albite, often arranged in fine bands (Albers, 2005). However, available data on the dissolution kinetics of albite suggest that its resistance to pressure solution would be similar to quartz (e.g. Hellmann et al., 1997). Further experimental work is needed, however, on real quartz–mica and quartz–albite–mica fault rocks under

hydrothermal conditions in order to test the underlying microphysical model and predictions.

4.3. The importance of phyllonites to the MTL past and present

Phyllonites with apparently mylonitic textures that overprint cataclasites and localise subsequent displacements are increasingly being recognised in fault rock suites associated with crustal-scale faults where there is good independent evidence for long-term weakening, e.g. reactivated faults (Imber et al., 1997, 2001; Stewart et al., 2000), low angle normal faults (Collettini and Holdsworth, 2004) and foreland basement décollement thrusts (Wibberley, 2005). The development of such weak fault rocks could well explain the long-lived history of the MTL in SW Japan. Unfortunately, due to poor exposure, we do not know if significant amounts of phyllonitic fault rocks like those seen in the Fukaya River section are associated with the entire MTL fault zone. This is important, because any weakening effects will only be transmitted up-scale to affect the entire fault zone if a well-connected network of weak fault rock can form over length scales of 10s or 100s of kilometres (Holdsworth, 2004). It appears that this was able to happen during the Tertiary sinistral displacement history along the MTL, and during the initial stages of Quaternary dextral reactivation—as evidenced by the localisation of dextral folds and shearing into the phyllonites.

By contrast, the patterns of most recent displacement and seismicity in this region of Japan suggest that the MTL is currently no longer behaving as a weak structure. Current seismic activity along the entire MTL across SW Japan is relatively low and, as a result, no linear distribution of microearthquakes is found along the fault trace (Okano and Kimura, 1996), and no creep motion has been detected (Onoue et al., 2002). Speculatively, it is possible that the relatively recent change to dextral motion has dismembered the previously mature, weak fault rock network established during millions of years of sinistral motion, leading to a general locking-up and strengthening of the MTL in SW Japan.

5. Conclusions

Structural, mineralogical and geochemical studies from the core region of the MTL show that early ultramylonites derived from Ryoke granitoids provide the protolith to the other fault rocks preserved. Cataclasis and fluid-driven feldspar alteration to phengite and precipitation of chlorite resulted in the sequential generation of cataclasite, foliated cataclasite and ultimately phyllonite, with increasing localisation of deformation at each stage. Widespread microstructural evidence for the operation of pressure solution processes in the foliated cataclasites and phyllonites highlights the dominant role of fluid-assisted viscous creep deformation mechanisms in these rocks.

The microphysical model of Bos and Spiers (2002) and Niemeijer and Spiers (in press) for combined frictional–viscous creep in quartz–mica phyllonites has been used to generate a strength profile for conditions appropriate to deformation along the MTL. This profile illustrates that very significant weakening is likely over long timescales, illustrating that phyllonites potentially play a key role in facilitating long-term weakening along crustal-scale faults. The findings of the present study will also be extremely relevant to the San Andreas Fault should foliated, phyllosilicate-rich fault rocks be found when drilling in the SAFOD experiment penetrates the fault core at 4 km depth.

Acknowledgements

SJ acknowledges receipt of a NERC studentship (NER/S/A/2001/06126) and REH funding from the Royal Society. The staff at the Sanrinsha Inn, Haze village, are thanked for their kindness, help and support during field seasons. E. Condliffe, N. Marsh and R. Kelly provided invaluable help and support during SEM and analytical work. Finally, we thank H. Takagi, K. Kanagawa and J. Hippertt for their helpful and detailed comments as reviewers.

References

Albers, M., 2005. Microscale kinematics and deformation mechanisms in phyllonitic mylonites and implications for the strength of continental fault zones. PhD/MSc research thesis. University of Utrecht, Faculty of Geosciences.

Bos, B., Spiers, C.J., 2000. Effect of phyllosilicates on fluid-assisted healing of gouge-bearing faults. Earth and Planetary Science Letters 184, 199–210.

Bos, B., Spiers, C.J., 2002. Frictional–viscous flow of phyllosilicate-bearing fault rock: microphysical model and implications for crustal strength profiles. Journal of Geophysical Research 107 (B2), 2028.

Bos, B., Peach, C.J., Spiers, C.J., 2000a. Slip behaviour of simulated gouge-bearing faults under conditions favouring pressure solution. Journal of Geophysical Research 105, 16699–16717.

Bos, B., Peach, C.J., Spiers, C.J., 2000b. Frictional–viscous flow of simulated fault gouge caused by the combined effects of phyllosilicates and pressure solution. Tectonophysics 327, 173–194.

Byerlee, J., 1990. Friction, overpressure and fault normal compression. Geophysical Research Letters 17, 2109–2112.

Cathelineau, M., 1988. Cation site occupancy in chlorites and illites as a function of temperature. Clay Minerals 23, 471–485.

Chester, F.M., Evans, J.P., Biegel, R.L., 1993. Internal structure and weakening mechanisms of the San Andreas fault. Journal of Geophysical Research 98, 771–786.

Collettini, C., Holdsworth, R.E., 2004. Fault zone weakening and character of slip along low-angle normal faults; insights from the Zuccale Fault, Elba, Italy. Journal of the Geological Society, London 161, 1039–1051.

Dallmeyer, R.D., Takasu, A., Yamaguchi, K., 1995. Mesozoic tectonothermal development of the Sambagawa, Mikabu and Chichibu belts, southwest Japan: evidence from ^{40}Ar–^{39}Ar whole-rock phyllite ages. Journal of Metamorphic Geology 13, 217–286.

Enami, M., Wallis, S.R., Banno, Y., 1994. Paragenesis of sodic pyroxene-bearing quartz schists: implications for the P–T history of the Sambagawa belt. Contributions to Mineralogy and Petrology 116, 182–198.

Goodwin, L.B., Wenk, H.R., 1995. Development of phyllonite from Granodiorite: mechanisms of grain-size reduction in the Santa Rosa mylonite zone, California. Journal of Structural Geology 17, 689–707.

Gueydan, F., Leroy, Y.M., Jolivet, L., Agard, P., 2003. Analysis of continental midcrustal strain localisation induced by microfracturing and reaction-softening. Journal of Geophysical Research 108 (B2, 2064), doi:10.1029/2001JB000611.

Hara, I., Shyoji, K., Sakurai, Y., Yokoyama, S., Hide, K., 1980. Origin of the Median Tectonic Line and its initial shape. Memoirs of the Geological Society of Japan 18, 27–49.

Hayama, Y., Yamada, T., 1980. Median Tectonic Line at the stage of its origin in relation to plutonism and mylonitisation in the Ryoke Belt. Memoirs Geological Society, Japan 18, 5–26.

Hellmann, R., Dran, J.C., Della Mea, G., 1997. The albite–water system: Part III. Characterization of leached and hydrogen-enriched layers formed at 300°C using MeV ion beam techniques. Geochimica et Cosmochimica Acta 61, 1575–1594.

Hickman, S., Sibson, R., Bruhn, R., 1995. Mechanical involvement off fluids in faulting. Journal of Geophysical Research 100, 12831–12840.

Hippertt, J.F., 1998. Breakdown of feldspar, volume gain and lateral mass transfer during mylonitisation of granitoids in a low metamorphic grade shear zone. Journal of Structural Geology 20, 175–193.

Holdsworth, R.E., 2004. Weak faults—rotten cores. Science 303, 181–182.

Holdsworth, R.E., Stewart, M., Imber, J., Strachan, R.A., 2001. The structure and rheological evolution of reactivated continental fault zones: a review and case study. In: Miller, J.A., Holdsworth, R.E., Buick, I.S., Hand, M. (Eds.), Continental Reactivation and Reworking. Geological Society, London, Special Publication 184, pp. 115–137.

Ichikawa, K., 1980. Geohistory of the Median Tectonic Line of Southwest Japan. Memoir of the Geological Survey of Japan 18, 187–212.

Imber, J., Holdsworth, R.E., Butler, C.A., Lloyd, G.E., 1997. Fault-zone weakening processes along the reactivated Outer Hebrides Fault Zone, Scotland. Journal of the Geological Society London 154, 105–109.

Imber, J., Holdsworth, R.E., Butler, C.A., Strachan, R.A., 2001. A reappraisal of the Sibson–Scholz fault zone model: the nature of the frictional to viscous ("brittle–ductile") transition along a long-lived, crustal-scale fault, Outer Hebrides, Scotland. Tectonics 20 (5), 601–624.

Ito, M., 1978. Granitic rocks and mylonitisation in the Kayumi district Mie Prefecture. MTL 3, 99–101.

Ito, T., Ikawa, T., Yamakita, S., Maeda, T., 1996. Gently north-dipping Median Tectonic Line (MTL) revealed by recent seismic reflection studies, southwest Japan. Tectonophysics 264, 51–63.

Janecke, S.U., Evans, J.P., 1988. Feldspar-influenced rock rheologies. Geology 16, 1064–1067.

Kronenberg, A.K., Segall, P., Wolf, G.H., 1990. Hydrolytic weakening and penetrative deformation within a natural shear zone. In: Duba, A.G., Durham, W.B., Handin, J.W., Wang, H.F. (Eds.), The Brittle–Ductile Transition in Rocks. Geophysical Monograph 56, pp. 21–36.

Lachenbruch, A.H., Sass, J.H., 1980. Heat flow and energetics of the San Andreas fault zone. Journal of Geophysical Research 85, 6185–6223.

Mares, V.M., Kronenberg, A.K., 1993. Experimental deformation of muscovite. Journal of Structural Geology 15 (9/10), 1061–1075.

Michibayashi, K., Masuda, T., 1993. Shearing during progressive retrogression in granitoids: abrupt grain size reduction of quartz at the plastic–brittle transition for feldspar. Journal Structural Geology 222, 151–164.

Mitra, G., 1984. Brittle to ductile transition due to large strains along the White Rock Thrust, Wind River Mountains, Wyoming. Journal of Structural Geology 6, 51–61.

Morrow, C., Radney, B., Byerlee, J.D., 1992. Frictional Strength and the Effective Pressure Law of Montmorillonite and Illite Clays. Fault Mechanics and Transport Properties of Rocks. Academic Press, San Diego, CA, pp. 69–88.

Niemeijer, A.R., Spiers, C.J., 2005. Influence of phyllosilicates on fault strength in the brittle–ductile transition: insights from rock analogue experiments. In: Bruhn, D., Burlini, L. (Eds.), Microstructural Evolution and Physical Properties in High Strain Zones. Geological Society, London, Special Publications, 245, 303–327.

Ohmoto, Y., 1993. Origin of the Median Tectonic Line. Journal of Science of the Hiroshima University 9, 611–669.

Okano, K., Kimura, S., 1996. Crustal movements in and around Shikoku, southwest Japan associated with great Nankai earthquakes. Journal of the Seismological Society, Japan 49, 361–374 (in Japanese).

Onoue, K., Hoso, Y., Fujita, Y., Doi, H., Tanaka, T., 2002. Electro-optical measurements on Median Tectonic Line. Annals of Disaster Prevention Research Institute, Kyoto University 45B, 525–533.

Rice, J.R., 1992. Fault stress states, pore pressure distributions, and the weakness of the San Andreas Fault. In: Evans, B., Wong, T.-F. (Eds.), Fault Mechanics and Transport Properties in Rocks. Academic Press, London, pp. 475–503.

Rutter, E.H., Holdsworth, R.E., Knipe, R.J., 2001. The nature and tectonic significance of fault zone weakening: an introduction. In: Holdsworth, R.E., Strachan, R.A., Magloughlin, J.F., Knipe, R.J. (Eds.), The Nature and Tectonic Significance of Fault Zone Weakening. Geological Society Special Publication 186, pp. 1–12.

Sakakibara, N., 1995. Structural evolution of multiple ductile shear zone system in the Ryoke belt, Kinki Province. Journal of Science of the Hiroshima University 10, 267–332.

Schmid, S.M., Handy, M.R., 1991. Towards a genetic classification of fault rocks: geological usage and tectonophysical implications. In: Müller, D.W., McKenzie, J.A., Weissert, H. (Eds.), Controversies in Modern Geology. Academic Press, London, pp. 339–361.

Scholz, C.H., 1990. The Mechanisms of Earthquakes and Faulting. Cambridge University Press, New York. 439pp.

Scholz, C.H., 2000. Evidence for a strong San Andreas fault. Geology 28, 163–166.

Shea, W.T., Kronenberg, A.K., 1992. Rheology and deformation mechanisms of isotropic mica schist. Journal of Geophysical Research 97, 15201–15237.

Shea, W.T., Kronenberg, A.K., 1993. Strength and anisotropy of foliated rocks with varied mica contents. Journal of Structural Geology 15, 1097–1121.

Shimada, K., Takagi, H., Osawa, H., 1998. Geotectonic evolution in transpressional regime: time and space relationships between mylonitisation and folding in the southern Ryoke belt, eastern Kii Peninsula, southwest Japan. Journal of the Geological Society of Japan 104, 825–844 (in Japanese with English abstract).

Shimada, K., Takagi, H., Suwa, K., Hayashida, M., 1999. The Median Tectonic Line and deformation of Ryoke Belt, Kii Peninsula. Field excursion guide (in Japanese). Contact: Koji Shimada, Division of Geology, Graduate School of Science and Engineering, Waseda University, Shinjuku, Tokyo 169-8050, Japan.

Sibson, R.H., 1977. Fault rocks and fault mechanisms. Journal of the Geological Society, London 133, 191–213.

Snoke, A.W., Tullis, J., Todd, V.R., 1998. Fault-Related Rocks: a Photographic Atlas. Princeton University Press, Princeton, NJ. 613pp.

Stewart, M., Holdsworth, R.E., Strachan, R.A., 2000. Deformation processes and weakening mechanisms within the frictional–viscous transition zone of major crustal-scale faults: insights from the Great Glen Fault Zone, Scotland. Journal of Structural Geology 22, 543–560.

Sugiyama, Y., 1992. Neotectonics of the forearc zone and the Setouchi Province in southwest Japan. Memoirs of the Geological Society of Japan 40, 219–223 (Japanese with English abstract).

Takagi, H., 1985. Mylonitic rocks of the Ryoke belt in the Kayumi area, eastern part of the Kii Peninsula. Journal of Geological Society, Japan 91, 637–651.

Takagi, H., 1986. Implications of mylonitic microstructures for the geotectonic evolution of the Median Tectonic Line, central Japan. Journal of Structural Geology 8, 3–14.

Takagi, H., Shibata, K., Sugiyama, Y., Uchiumi, S., Matsumoto, A., 1989. Isotopic ages of rocks along the Median Tectonic Line in the Kayumi area, Mie Prefecture. Journal of Petrology, Mineralogy and Economic Geology 84, 74–88 (in Japanese with English abstract).

Van Staal, C.R., Rogers, N., Taylor, B.E., 2001. Formation of low-temperature mylonites and phyllonites by alkali-metasomatism weakening of felsic volcanic rocks during progressive, subduction-related deformation. Journal of Structural Geology 23, 903–921.

Wallis, S., Banno, S., Radvanec, M., 1992. Kinematics, structure and relationship to metamorphism of east–west flow in the Sambagawa belt, southwest Japan. The Island Arc 1, 176–185.

Wang, C.-Y., 1984. On the constitution of the San Andreas fault zone in central California. Journal of Geophysical Research 89, 5858–5866.

White, S.H., Burrows, S.E., Carreras, J., Shaw, N.D., Humphreys, F.J., 1980. On mylonites in ductile shear zones. Journal of Structural Geology 2, 165–187.

Wibberley, C.A.J., 1999. Are feldspar-to-mica reactions necessarily reaction-softening processes in fault zones? Journal of Structural Geology 21, 1219–1227.

Wibberley, C.A.J., 2005. Initiation of basement thrust detachments by fault-zone reaction weakening. In: Bruhn, D., Burlini, L. (Eds.), High Strain Zones: Structure and Physical Properties. Geological Society Special Publication 245, pp. 347–372.

Wibberley, C.A.J., Shimamoto, T., 2003. Internal structure and permeability of major-slip fault zones: the Median Tectonic Line in Mie Prefecture, Southwest Japan. Journal of Structural Geology 25, 59–78.

Wintsch, R.P., Christofferson, R., Kronenberg, A.K., 1995. Fluid-rock reaction weakening of fault zones. Journal of Geophysical Research 100, 13021–13032.

Yamamoto, H., Masuda, T., 1987. Horizontal ductile shearing in mylonites of the Ryoke Belt in the Misakubo district, northwest Shizuoka Prefecture. Abstract 94th Annual Meeting Geological Society, Japan, 452pp.

Zoback, M.D., 2000. Strength of the San Andreas. Nature 405, 31–32.